State-to-state dissociation of OClO($\tilde{A}\ ^2A_2\nu_1$,0,0)→ClO($X\ ^2\Pi_\Omega, v, J$)+O(^3P)

Ralph Felix Delmdahl, Stephan Baumgärtel, and Karl-Heinz Gericke
Institut für Physikalische und Theoretische Chemie, Johann Wolfgang Goethe-Universität Frankfurt/Main, Marie-Curie-Strasse 11, D-60439 Frankfurt/Main, Germany

(Received 12 June 1995; accepted 6 November 1995)

Applying the two-photon laser-induced fluorescence technique for nascent state resolved ClO($X\ ^2\Pi_\Omega, v, J$) detection, the photofragmentation dynamics of OClO in the ($\tilde{A}\ ^2A_2$11,0,0) and the ($\tilde{A}\ ^2A_2$18,0,0) state is investigated at fixed photolysis wavelengths of 351 nm and 308 nm. In both experiments the product fragments are formed in their electronic ground states, namely ClO($^2\Pi_\Omega$) and O(^3P). A complete product state analysis proves the ClO radicals originating from the OClO($\tilde{A}\ ^2A_2$11,0,0) dissociation at 351 nm to be formed in $v=0-4$ vibrational states with a spin–orbit ratio of $P(^2\Pi_{3/2}):P(^2\Pi_{1/2})=3.8\pm0.5$. The ClO fragment shows moderate rotational excitation. The obtained ClO product state distributions and the relatively high translational energy of the fragments can be explained by predissociation of the ($\tilde{A}\ ^2A_2\nu_1$,0,0)-excited parent molecule in the course of which the initial symmetric stretch motion (ν_1) of OClO is transferred into the dissociative asymmetric stretching mode (ν_3). ClO line profile measurements indicate a dissociation time of less than 0.5 ps. Resulting from the OClO($\tilde{A}\ ^2A_2$18,0,0) dissociation at 308 nm ClO is generated in very high vibrational states. The rotational excitation is comparable to that of the 351 nm photolysis study. © *1996 American Institute of Physics.* [S0021-9606(96)00307-5]

I. INTRODUCTION

By now, it is a well-known fact that the polar stratospheric ozone destruction is caused on a large scale by the photochemistry of chlorine oxides.[1–4]

In recent years, numerous attempts have been made to understand the gas phase dynamics of OClO photodissociation from the first absorption band.[5–11] This near-UV absorption spectrum extending from about 260 to 480 nm results from the ($\tilde{A}\ ^2A_2\nu_1,\nu_2,\nu_3\leftarrow\tilde{X}\ ^2B_1$0,0,0) electronic transition and shows considerable vibrational structure including progressions of all three vibrational modes. Two decomposition pathways are observable for the ($\tilde{A}\ ^2A_2$)-excited parent molecule leading to formation of ClO+O (major channel) and $Cl+O_2$ (minor channel), respectively. As examined by Davis and Lee,[9] the yield of the $Cl+O_2$ product channel reaches a maximum of $3.9\pm0.8\%$ at a photolysis wavelength of 404 nm and decreases at shorter wavelengths (e.g., $<0.2\%$ in the range of 350–370 nm). Furthermore, a strong sensitivity to the initial vibrational state of the electronically excited OClO molecule is seen in the branching ratio for the two product channels.[9,16] Davis and Lee[9] found the formation of ClO tenfold greater from OClO with asymmetric stretching (ν_3) excitation than from neighboring vibrational states with pure symmetric stretching (ν_1) excitation or symmetric stretching and bending (ν_2) excitation. Bishenden and Donaldson[16] also reported that asymmetric stretching excitation enhances the ClO production. A previously assumed photoisomerization mechanism in the gas phase leading to asymmetric ClOO and subsequently to formation of $Cl+O_2$,[5,6] as obtained almost quantitatively from matrix-isolated OClO molecules,[12] has been shown to be extremely unlikely under gaseous conditions and can therefore be excluded.[9] In our work, the ClO+O product channel predominating in the near-UV OClO photofragmentation is the subject of investigation. In their one-color resonance-enhanced multiphoton ionization (REMPI) spectra between 335 and 370 nm, Vaida *et al.* observed ClO from dissociation of ($\tilde{A}\ ^2A_2$)-excited OClO in $v=3-6$ vibrational states.[6,8] However, ionic fragmentation of $OClO^+$ cannot be entirely ruled out in this experiment. Recent results of Baumgärtel and Gericke,[13] who applied the two-photon laser-induced fluorescence ($2h\nu$) LIF technique for ClO detection, indicate that in the one-color near-UV photodissociation of OClO the fragments are formed mainly in lower vibrational states.

Contrary to an early unsuccessful attempt in detecting the ClO radical by the conventional one-photon LIF method probing the predissociative ($A\ ^2\Sigma$) state of ClO,[14] the ($2h\nu$) LIF technique uses the high-lying radiative ($C\ ^2\Sigma$) Rydberg state by two-photon excitation of nascent ClO($X\ ^2\Pi_\Omega, v, J$) fragments. With a more intricate experimental setup the ($C\ ^2\Sigma$) state is also attainable in ($1h\nu$) LIF detection of ClO fragments in the VUV region using four-wave mixing as reported recently by Matsumi *et al.*[15] Although ($2h\nu$) LIF represents an excellent way to achieve both vibrational and rotational ClO spectral resolution, the one-color experiment in the photodissociation of OClO still suffers from a particular disadvantage.

As a consequence of scanning the photolysis wavelength over a range of around 30 nm with regard to the absorption spectrum of OClO, approximately ten different vibrational ($\tilde{A}\ ^2A_2\nu_1,\nu_2,\nu_3$) states are passed. Under these conditions, the initial state from which the photodissociation occurs is in no way determined. However, it is an indelible fact that a deep insight into the fragmentation dynamics is only available if a state-to-state experiment, requiring both the knowledge of the initial and the final state, is carried out.

In order to meet this necessity, the OClO photodissociation reported in this paper is performed using constant wave-

Downloaded¬08¬Jan¬2002¬to¬134.169.41.178.¬Redistribution¬subject¬to¬AIP¬license¬or¬copyright,¬see¬http://ojps.aip.org/jcpo/jcpcr.jsp

lengths of either 351 nm or 308 nm, exciting ($\tilde{X}\ ^2B_1 0,0,0$) ground state OClO either into the ($\tilde{A}\ ^2A_2 11,0,0$) or into the ($\tilde{A}\ ^2A_2 18,0,0$) state. Thus, the photo-induced decay of the parent molecule is initiated at these particular photolysis wavelengths by sole contribution of the symmetric stretching mode (ν_1). Bishenden and Donaldson[16] also detected ClO originating from distinct ($\tilde{A}\ ^2A_2 \nu_1,\nu_2,\nu_3$) states of the OClO parent molecule using a two-color REMPI experiment. At a photolysis wavelength of 360 nm corresponding to ($\tilde{A}\ ^2A_2 10,0,0$)-excited OClO, they obtained (2+1) REMPI spectra which indicate vibrational excitation of the ClO fragments. However, the assignment of the observed transitions proved to be a rather challenging task because three close-lying electronic states, namely the D, E, and F state of ClO, were involved in the spectral features. Therefore, the exact determination of neither the vibrational nor the rotational product state distribution was possible.

In the two-color ($2h\nu$) LIF experiments described in this work, the elementary dissociation process of ($\tilde{A}\ ^2A_2 \nu_1,0,0$)-excited OClO is investigated by the complete product state analysis and by comparing the obtained results with *ab initio* calculations of the upper potential surfaces.[17]

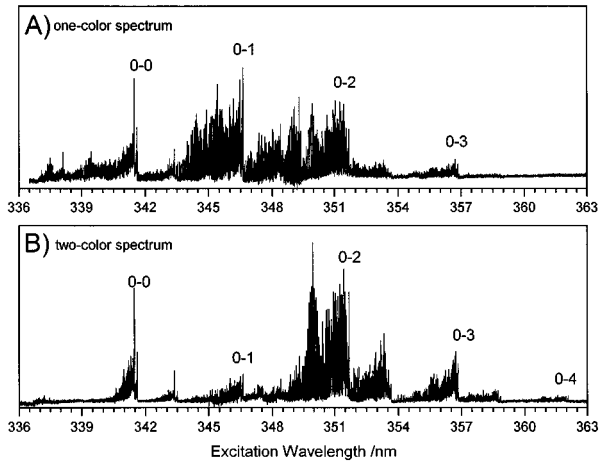

FIG. 1. (a) Two-photon laser-induced fluorescence spectrum of ClO originating from the OClO photolysis in a one-color experiment. (b) Two-color ($2h\nu$) LIF spectrum of ClO. The photolysis wavelength is fixed at 351 nm, corresponding to an initial decay originating definitely from the excited ($\tilde{A}\ ^2A_2,11,0,0$) state of the parent molecule.

II. EXPERIMENTAL DETAILS

According to the method of Derby and Hutchinson[18] OClO was generated by pouring a 10% Cl_2/N_2 mixture through a column containing $NaClO_2$ and glass beads. The actual yield of OClO was at least 70% as indicated by absorption measurements. Since the remainders, being Cl_2 and N_2, show no influence on further events, the yellow product was transferred to the photo-process without further steps of purification.

A XeF excimer laser (Lambda Physik EMG 201 MSC) provided a photolysis wavelength of 351 nm. The OClO photolysis at 308 nm was carried out with a XeCl excimer laser (Lambda Physik EMG 101 MSC). The output energy of the photolysis lasers was about 150 mJ of which 10% reached the interior of the reaction chamber. A beam diameter of 0.02 cm^2 and the corresponding OClO absorption coefficients which are reported in Ref. 19 guaranteed the photolysis proceeding at saturation. When the probe laser was blocked, ClO fragments were not observable in the focus of only the photolysis laser. Furthermore, a variation of the photolysis laser energy had no influence on the intensity of the observed LIF signals. This fact and the relatively low photolysis energy of around 15 mJ in the reaction cell gives evidence against our LIF signals resulting from multiphoton processes. The probe energy of the tunable detection system consisting of a dye laser (Lambda Physik FL 3002) pumped by a XeCl excimer laser (Lambda Physik LPX 100) was 5–10 mJ, depending on the respective wavelength. The spectral extent of the observable ClO ($C\ ^2\Sigma \leftarrow X\ ^2\Pi_\Omega$) rovibronic transitions required the usage of p-terphenyl in dioxane and RDC 360-neu (Radiant Dyes Laser & Acc. GmbH) in dioxane as active laser media. A quartz lens ($f=500$ mm) was employed to focus the photolysis beam into the reaction chamber. Counterpropagating and time delayed, the detection beam entered the chamber focused in the same way by a quartz lens ($f=500$ mm). At this point, the total enclosure of the detection beam by the photolysis beam volume inside the reaction cell was of great importance for providing actual two-color experimental conditions. The dye laser bandwidth of 0.4 cm^{-1} was optionally reducible to 0.08 cm^{-1} by additional application of an intracavity étalon (Lambda Physik), as necessary for rotational linewidth and Doppler profile measurements.

The ($2h\nu$) LIF spectrum [Fig. 1(b)] resulting from the 351 nm photolysis was recorded at a total cell pressure of 45 Pa and 100 ns delay between photolysis and detection. Hence, collisions and secondary reactions affecting the nascent photolysis products were prevented and nascent product state distributions were observable.

A solar-blind photomultiplier tube (EMR 542G-08-18) perpendicular to the laserbeams registered the fluorescence light in the region of around 170 nm originating from ($C\ ^2\Sigma$)-excited ClO radicals. The multiplier output signal was integrated by a boxcar integrator and averager (Stanford Research Systems SR 250) and after A/D conversion recorded by a personal computer (Siemens PC AT 386), the latter also controlling the stepping motor for both grating and étalon. Simultaneous recording of fluorescence as well as laser intensity allowed to obtain normalized spectra. A home made trigger device regulated the order of events. The jitter between the photolysis and detection laser pulse was about 10 ns, primarily determined by the excimer laser.

At the photolysis wavelength of 308 nm a pressure of 200 Pa with 200 ns delay was additionally used. Under these experimental conditions, the rotational state distribution is influenced by collision processes whereas the fragment vibration is unaffected. This was necessary because the spectral features of the observable lower ($0 \leftarrow v$)-transitions decreased as a consequence of the stronger vibronic excitation of the fragments. Since the generation of vibrationally ex-

Downloaded¬08¬Jan¬2002¬to¬134.169.41.178.¬Redistribution¬subject¬to¬AIP¬license¬or¬copyright,¬see¬http://ojps.aip.org/jcpo/jcpcr.jsp

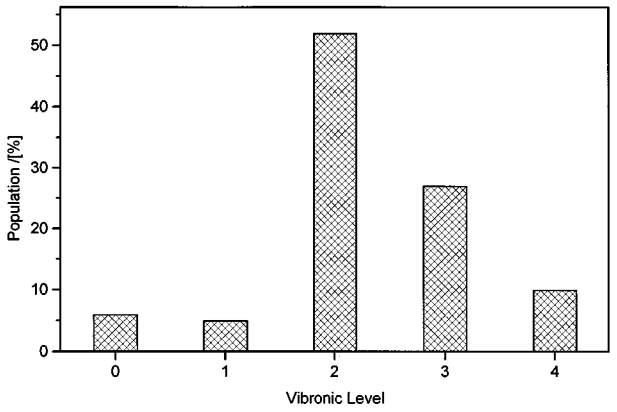

FIG. 2. Vibrational product state distribution of the ClO ($X\ ^2\Pi_\Omega$) radicals generated in the 351 nm photodissociation of OClO.

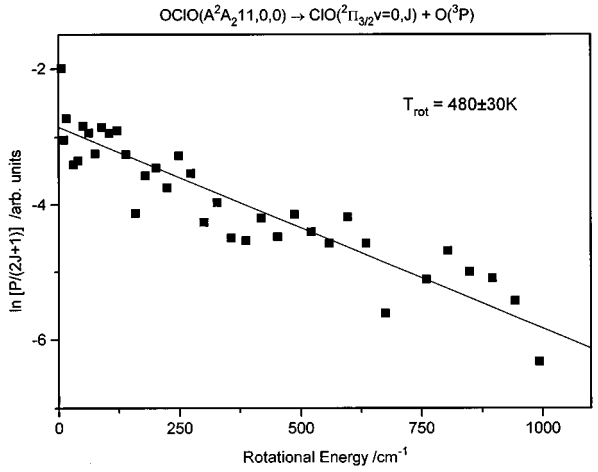

FIG. 3. Boltzmann plot of the (0-0, $\Omega=3/2$)-transition in Fig. 1(b).

cited ClO up to $v=17$ is energetically possible in the 308 nm photolysis, the vibrational distribution of ClO including higher vibronic levels was further investigated in an additional two-color (2+1)-REMPI/TOF (time-of-flight) experiment.[20] OClO was prepared as described above and carried to photolysis via a pulsed molecular beam nozzle. The O(^3P) partner fragments generated at a photolysis wavelength of 308 nm were detected by resonant two-photon excitation of the $2p\ ^3P_2 \rightarrow 3p\ ^3P_J(J=0,1,2)$ transition[21] and subsequent ionization by an additional photon at a detection wavelength of 226 nm. The signal of the ions drifting to the detector was then recorded. The pressure in the reaction chamber was around 5×10^{-3} Pa allowing the measurement of the nascent translational energy distribution. A detailed description of the experimental apparatus is given in Ref. 22.

III. RESULTS

In Fig. 1(a) the one-color ($2h\nu$) LIF spectrum is shown. The very efficient laser dye RDC 360-neu (Radiant Dyes Laser & Acc. GmbH) was employed, resulting in higher intensities for the (0←2)- and the (0←3)-band in comparison to the recently reported one-color experiment.[13] The normalized ($2h\nu$) LIF spectrum of nascent ClO resulting from the two-color experimental setup at a fixed OClO photolysis wavelength of 351 nm is depicted in Fig. 1(b). Solely ($0\leftarrow v$)-transitions are observed. The assignment of the appearing spectral features is possible by comparison with the simulated rovibrational transitions. Quite obviously, a significant difference exists between this spectrum and that obtained from the one-color experiment in Fig. 1(a). In the one-color OClO photodissociation, the ClO fragments are formed mainly in lower vibrational states whereas the fragmentation process of OClO in the ($\tilde{A}\ ^2A_2$11,0,0) state leads to ClO radicals which are vibrationally hot.

TABLE I. Franck–Condon factors, populations, and spin–orbit ratios of the observed vibrational transitions in the photolysis of OClO at 351 nm.

$v'\leftarrow v$	FC[a]	$P(v)_{exp}$/%	$P(v)^{b}_{Prior}$/%	$P(\Pi_{3/2}):P(\Pi_{1/2})$
0←0	0.3107	6	20	4.32
0←1	0.3412	5	17	(3.81)
0←2	0.2074	52	15	3.76
0←3	0.0924	27	13	3.35
0←4	0.0336	10	10	(3.81)

[a]Reference 23.
[b]Rigid rotator harmonic oscillator (RRHO) approximation.

The quantitative evaluation of the vibrational features in Fig. 1 is based on the following consideration. The dependence of the intensity of an isolated transition $(v',J')\leftarrow(v,J)$ on both the transition probability and the initial population of the respective rovibronic level (v,J) is given by

$$I^{v'v}_{J'J} \propto B^{v'v}_{J'J} \cdot P(v,J). \tag{1}$$

The desired vibrational populations $P(v)$ are obtained by integrating over the entire rotational envelope of the respective vibrational band

$$\int_{\nu(v'v)} I^{v'v}_{J'J}(\nu)\,d\nu \propto \cdot \mathrm{FC}(v'v)\cdot P(v), \tag{2}$$

at which FC($v'v$) describes the corresponding Franck–Condon factors of the ClO ($C\leftarrow X$) vibrational transitions which are taken from Ref. 23.

Figure 2 shows that the vibrational state distribution of nascent ClO is inverted, possessing a maximum population at $v=2$. The vibrational product state distribution, the employed Franck–Condon factors as well as the ratio of the populations of the spin–orbit systems are listed in Table I.

The population ratios of the spin–orbit systems are obtained by separate integration over the corresponding lines. Concerning the spin–orbit subbands of the (0←0)-, (0←2)-, and the (0←3)-vibronic transition; the population ratios $P(^2\Pi_{3/2}):P(^2\Pi_{1/2})$ are readily obtainable from the spectral features. The (0←1, $\Omega=3/2$)-subband is partially covered by the (0←2)-transition and the (0←4, $\Omega=3/2$)-subband is too weak. Since the obtained values of the populations of the spin–orbit ratios are identical within the limit of error, similar conditions are assumed in the case of the (0←1)- and the (0←4)-transition. Thus, in the OClO photolysis at 351 nm

Downloaded¬08¬Jan¬2002¬to¬134.169.41.178.¬Redistribution¬subject¬to¬AIP¬license¬or¬copyright,¬see¬http://ojps.aip.org/jcpo/jcpcr.jsp

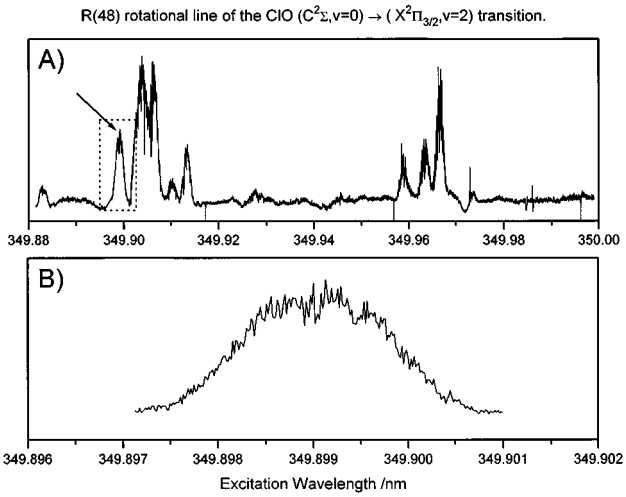

FIG. 4. (a) High resolution scan of the (0-2, $\Omega=3/2$)-transition obtained from the two-color experiment at 351 nm. The application of an etalon reduced the laser bandwidth to 0.08 cm^{-1}. (b) Enlarged view of the $R(48)$ rotational line, which is marked in (a). The analysis of the Doppler profile yielded an upper limit of 0.5 ps for the lifetime of the excited OClO molecule.

the ClO spin–orbit system $\Omega=3/2$ is preferred with a population ratio $P(^2\Pi_{3/2}):P(^2\Pi_{1/2})$ of 3.8 ± 0.5. In addition, the $(2h\nu)$ LIF spectrum of the single ClO ($C\ ^2\Sigma$, $v'=0\leftarrow X\ ^2\Pi_\Omega$, $v=0$) transition recorded under completely rotationally and vibrationally relaxed conditions (30 μs delay and 2 kPa) yields a ratio of 4.00. This result is in good agreement with the theoretically expected $P(^2\Pi_{3/2}):P(^2\Pi_{1/2})$ value of 4.5 calculated for a Boltzmann distribution at 300 K. The spectroscopic properties of the ClO radical applicable for two-photon excitation are described in the previous work.[13]

In obtaining the rotational state distributions simulated vibrational bands are adapted to the measured ones using a least square fit procedure. The theoretical intensity at a frequency ν is given by

$$I_{\text{theo}}(\nu)\propto\sum_{q',q}P(q)\cdot S_{q'q}\cdot L(\nu_{q'q}-\nu,\Delta\nu), \tag{3}$$

in which $P(q)$ is the desired quantum state population, $S_{q'q}$ the transition probability, and $L(\nu_{q'q}-\nu,\Delta\nu)$ the Gaussian line shape function centered at $\nu_{q'q}$ and possessing a linewidth (FWHM) of $\Delta\nu$. Summation is carried out over all transitions $(q'\leftarrow q)$ contributing to the signal at the respective frequency. The population $P(q)$ of each quantum state q is obtainable in this way.

For the spin–orbit subband $\Omega=3/2$ of the $(0\leftarrow0)$-transition, the nascent population of rotational states is found to correspond to a Boltzmann distribution with a temperature parameter of 480 ± 30 K. The Boltzmann plot of nascent $ClO(X\ ^2\Pi_{3/2}, v=0)$ originating from the 351 nm photolysis is shown in Fig. 3. Unfortunately, precise molecular constants of the higher vibronic levels of the electronic $ClO(X\ ^2\Pi)$ ground state do not exist so far. Therefore, populations of rotational states belonging to $v>0$ are not available by a least square fit procedure but estimated as follows. The respective transitions are simulated using the ClO molecular constants which are measured by Coxon[24] assuming thermal rotational state distributions of different temperatures. The transitions calculated in this way are compared with the observed experimental features. In each case, the best correspondance is acquired at about 1000 ± 300 K.

A further experiment serves as an indication for the adequacy of the applied $(2h\nu)$ LIF method. Selecting a delay of 30 μs between photolysis and ClO detection and increasing the total cell pressure with argon up to 2 kPa should lead to sole observation of completely relaxed product molecules; in particular, this means no vibronic excitation as well as a rotational state distribution corresponding to that at room temperature. Both exclusive appearance of the $(0\leftarrow0)$-transition and a very good agreement of obtained and expected rotational state distribution are found.

Figure 4(a) presents an enlarged part of the $(0\leftarrow2, \Omega=3/2)$-transition of the spectrum in Fig. 1. The single $R(48)$ rotational line is depicted in Fig. 4(b). Each high resolution scan is recorded with the etalon equipped detection system at a reduced laser bandwidth of 0.08 cm^{-1}. The width as well as the shape of the Doppler profile of the $R(48)$ line are determined from a least square fit. The applied fit procedure which is described in Ref. 25 yields an experimental linewidth (FWHM) of 0.166 ± 0.01 cm^{-1}. This is in excellent agreement with the theoretically calculated linewidth of 0.163 cm^{-1} which is obtained by considering the available energy and the rotational energy of $J_{\text{ClO}}=48$.

From the line shape, the anisotropy parameter β is deduced,[25] giving evidence of the correlation between the molecular vectors $\boldsymbol{\mu}_{\text{parent}}$ and $\mathbf{v}_{\text{fragment}}$. An experimental value of $\beta_{\text{exp}}=1.14$ is obtained. Provided that the initial alignment between $\boldsymbol{\mu}_{\text{parent}}$ and $\mathbf{v}_{\text{fragment}}$ is fixed, a theoretical value $\beta_{\text{theo}}=1.73$ is calculated. The experimental parameter $\beta_{\text{exp}}=1.14$ resulting from the Doppler profile indicates that the initial $\boldsymbol{\mu}$, $\mathbf{v}$-correlation is influenced by the motion of the excited parent molecule during the fragmentation process. As described in Ref. 26, the deviation of the anisotropy parameter β from the theoretically expected value can be used to estimate the lifetime τ of the electronically excited parent molecule. A lifetime of $\tau=0.5$ ps is calculated for the $(\tilde{A}\ ^2A_2 11,0,0)$-excited OClO molecule. However, it is important to mention that geometrical rearrangements of the dissociation complex as well as coupling with the electronic $(^2A_1)$ and $(^2B_2)$ states also strongly reduce the β_{theo} parameter. As a consequence, the calculated lifetime presents an upper limit. Nevertheless, the obtained value is in agreement with recent OClO femtosecond investigations, in which the lifetime of $(\tilde{A}\ ^2A_2)$-excited OClO was measured to 0.5 ps.[27]

The photodissociation of OClO at a constant wavelength of 308 nm corresponds to a higher symmetric stretch (ν_1) excitation of the parent molecule. In this case, essentially $\nu_1=18$ and to a smaller extent $\nu_1=17$ is excited.[19] The nascent rotational state distributions which are observed in the 308 nm $(2h\nu)$ LIF spectrum at 45 Pa and 100 ns delay appear similar to those obtained from the 351 nm photolysis.

The vibrational product state distribution $P(v)$ of the ClO fragments for the five lowest vibrational levels is pre-

Downloaded¬08¬Jan¬2002¬to¬134.169.41.178.¬Redistribution¬subject¬to¬AIP¬license¬or¬copyright,¬see¬http://ojps.aip.org/jcpo/jcpcr.jsp

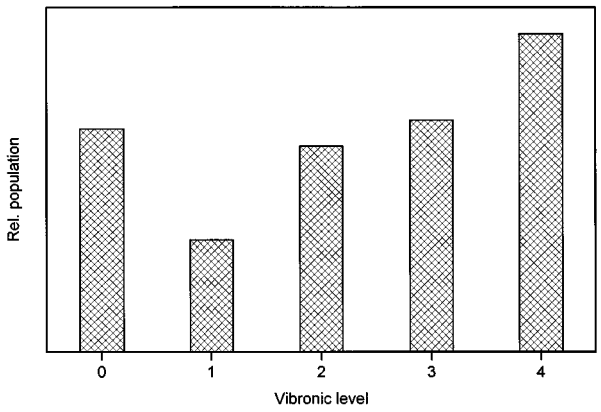

FIG. 5. Vibrational product state distribution of the first five vibronic levels of ClO as a result of the 308 nm OClO photolysis.

sented in Fig. 5. Except for the population of the $v=0$ vibronic level, the population of the vibrational states increases continually up to $v=4$. Higher vibronic levels are not observable because the increase of the population numbers is too weak to compensate the strongly decreasing Franck–Condon factors. However, the line intensities are significantly lower than those observed in the corresponding one-color spectrum, indicating the formation of rather strong vibronically excited ClO radicals.

In order to determine the ClO population in higher vibrational levels than $v=4$ a two-color REMPI/TOF study is performed at which the time-of-flight of the recoiled $O(^3P)$ atoms is measured. The internal energy distribution of ClO obtained from the observed time-of-flight distribution of the $O(^3P)$ partner fragments is represented in Fig. 6. Although the vibrational structure is not resolved, it is obvious from the spectrum that ClO with an internal energy of up to at least 8000 cm^{-1} is generated in the 308 nm photolysis. This result corresponds to ClO fragments which are significantly vibrationally excited and agrees with the tendency observed in the 308 nm $(2h\nu)$ LIF experiment. The kinetic energy of the O atoms corresponding to higher internal energies of ClO is too low and hence the ions are not detectable in the drift experiment. Detailed investigations of the OClO photolysis using the REMPI/TOF method are in progress and will be published elsewhere.[20]

IV. DISCUSSION

The ground state of OClO has the configuration in C_{2v} geometry[17]

$$\tilde{X}\ ^2B_1[^2A'']: \quad (5b_2)^2(8a_1)^2(1a_2)^2(3b_1)^1,$$

at which the term in square brackets $[^2A'']$ corresponds to C_s geometry of the molecule. The first three excited electronic states,

$$\tilde{A}\ ^2A_2[^2A'']: \quad (5b_2)^2(8a_1)^2(1a_2)^1(3b_1)^2,$$

$$^2A_1[^2A']: \quad (5b_2)^2(8a_1)^1(1a_2)^2(3b_1)^2,$$

$$^2B_2[^2A']: \quad (5b_2)^1(8a_1)^2(1a_2)^2(3b_1)^2,$$

involve excitation from the $1a_2$, $8a_1$, and $5b_2$ orbitals into the singly occupied $3b_1$ level. The transition from the $\tilde{X}\ ^2B_1$ state to the $^2B_2$ state is dipole forbidden in C_{2v} geometry. Both the $^2A_1 \leftarrow \tilde{X}\ ^2B_1$ and the $\tilde{A}\ ^2A_2 \leftarrow \tilde{X}\ ^2B_1$ transition are dipole allowed but the former is of perpendicular polarization and should be weak. In fact, spectroscopic experiments observe only excitation to the $\tilde{A}\ ^2A_2$ state.[6,8,10,27] The near-UV absorption spectrum of chlorine dioxide[28] shows sharp features originating from a strong progression of the symmetric stretching mode (ν_1) and combinations of the symmetric stretching mode with the bending mode (ν_2) and the asymmetric stretching mode (ν_3).

A look at the OClO UV absorption spectrum indicates that the applied photolysis wavelengths of both 351 nm and 308 nm exclusively affect the symmetric stretching mode (ν_1) of the $OClO(\tilde{A}\ ^2A_2)$ parent molecule. At 351 nm only $\nu_1=11$ and at 308 nm primarily $\nu_1=18$ participates in the excitation process. Resulting from this particular initial symmetric stretch excitation, the ClO radicals are formed in $v=0-4$ vibrational states for the 351 nm photolysis and significantly vibrationally hotter for the 308 nm photolysis. Both photolysis wavelengths generate the ClO fragments with moderate rotational excitation.

The available energy E_{av} which has to be released in the products of a photodissociation process is defined by

$$E_{av}=h\nu+E_{int}(OClO)-D_0, \tag{4}$$

in which $h\nu$ represents the energy of the photons used for the photolysis, $E_{int}(OClO)$ describes the initial internal energy of the parent molecule before excitation ($E_{int}\approx E_{rot}=3/2RT$) and D_0 is the dissociation energy of the OClO molecule. With a D_0 value of 231 ± 8 kJ/mol (Ref. 29) the energy available for the products at a photolysis wavelength of 351 nm amounts to 114 ± 8 kJ/mol. The complete product state analysis, i.e., the determination of the internal energy of the ClO

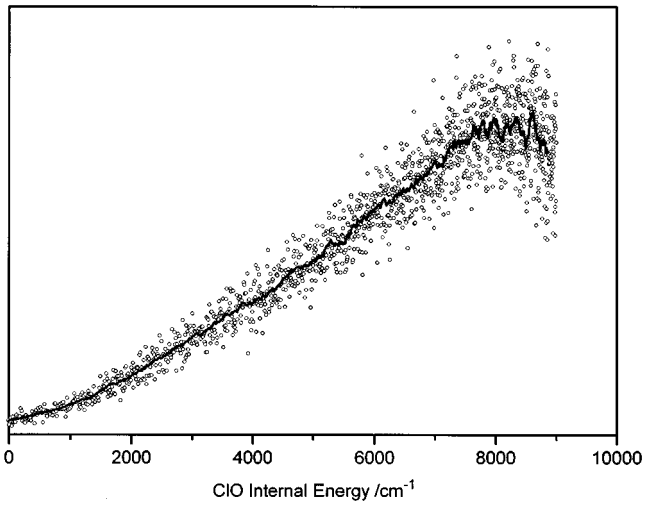

FIG. 6. Internal energy distribution of ClO obtained from the time-of-flight distribution of the $O(^3P)$ partner fragments. The recorded data points become uncertain beyond 8000 cm^{-1} due to very low recoil velocities of the $O(^3P)$ atoms corresponding to high internal excitation of the ClO fragments.

Downloaded¬08¬Jan¬2002¬to¬134.169.41.178.¬Redistribution¬subject¬to¬AIP¬license¬or¬copyright,¬see¬http://ojps.aip.org/jcpo/jcpcr.jsp

TABLE II. Distribution of the available energy over the fragments obtained in the state-to-state dissociation $OClO \rightarrow ClO\ (X\ ^2\Pi_\Omega, v, J) + O(^3P)$ at a constant photolysis wavelength of 351 nm (E_{av}=9540 cm^{-1}).

	$\langle E_{vib}\rangle$/cm^{-1}	$\langle E_{rot}\rangle$/cm^{-1}	$\langle E_{trans}\rangle$/cm^{-1}	f_{vib}/%	f_{rot}/%	f_{trans}/%
Experiment	1920	675	6945	20	7	73
Prior	2767	2767	4006	29	29	42

fragments, is possible for the 351 nm OClO photolysis. The distribution of the available energy over the degrees of freedom of the fragments originating from ($\tilde{A}\ ^2A_2 11,0,0$) excited OClO is summarized in Table II.

Provided that the internal energy of ClO is known, the measured linewidth (FWHM) of the rotational line depicted in Fig. 4(b) allows the determination of the dissociation energy of OClO. The Doppler width of the $R(48)$ transition is measured at 0.166±0.01 cm^{-1} correlating with a ClO velocity of 880±50 m/s and an O velocity of 2830±170 m/s, respectively. Thus, the entire translational energy of both fragments amounts to 84±10 kJ/mol leading to an E_{av} value of 121±10 kJ/mol and a D_0 value of 224±10 kJ/mol. The excellent agreement between D_0 determined from the $R(48)$ linewidth and the D_0 value (231±8 kJ/mol) in Ref. 29 additionally supports the application of the ($2h\nu$) LIF technique in the state-resolved detection of nascent ClO radicals.

Cuts through *ab initio* potential energy surfaces of the OClO molecule have been calculated by Werner *et al.*[17] and are shown in Fig. 7 with respect to the symmetric, the asymmetric bond length distortion, and the variation of the valence angle. The $\tilde{A}\ ^2A_2$, $^2A_1$, and $^2B_2$ surfaces are bonding with respect to both the symmetric O–Cl–O distance r_{ClO} and the valence angle. Asymmetric bond length distortion R_{ClO} leads to $O(^3P)+ClO(^2\Pi)$. However, both the $\tilde{A}\ ^2A_2$ [$^2A''$ in C_s geometry] and the $^2A_1$ [$^2A'$] surface exhibit a barrier and only the unbounded $^2B_2$ [$^2A'$] surface is repulsive with respect to R_{ClO} (Fig. 7). For this reason, at low excitation energies OClO can only decay on the $^2B_2$ [$^2A'$] surface and Peterson and Werner[17] proposed the following three-step fragmentation mechanism promoted by the asymmetric stretch: Internal conversion from the initially excited $\tilde{A}\ ^2A_2$ [$^2A''$] state to the $^2A_1$ [$^2A'$] state through spin–orbit coupling, followed by vibronic coupling of the $^2A_1$ [$^2A'$] state with the reactive $^2B_2$ [$^2A'$] state via the asymmetric stretch, and finally decay of OClO on the $^2B_2$ [$^2A'$] surface into the O+ClO fragments. Since the asymmetric stretch is the dissociative mode, excitation of combination bands of symmetric and antisymmetric stretch should promote the dissociation process. This behavior was experimentally observed.[9,16]

The $\tilde{A}\ ^2A_2$ surface which is directly reached in the present experiment exhibits a barrier of about 0.4 eV with respect to asymmetric bond length distortion. Since the minimum of the $\tilde{A}\ ^2A_2$ state is at 2.7 eV (right part of Fig. 7), energies above 3.1 eV may be sufficient to overcome that barrier. Indeed, the absorption spectrum of jet cooled OClO shows increasing homogeneous linewidth broadening with

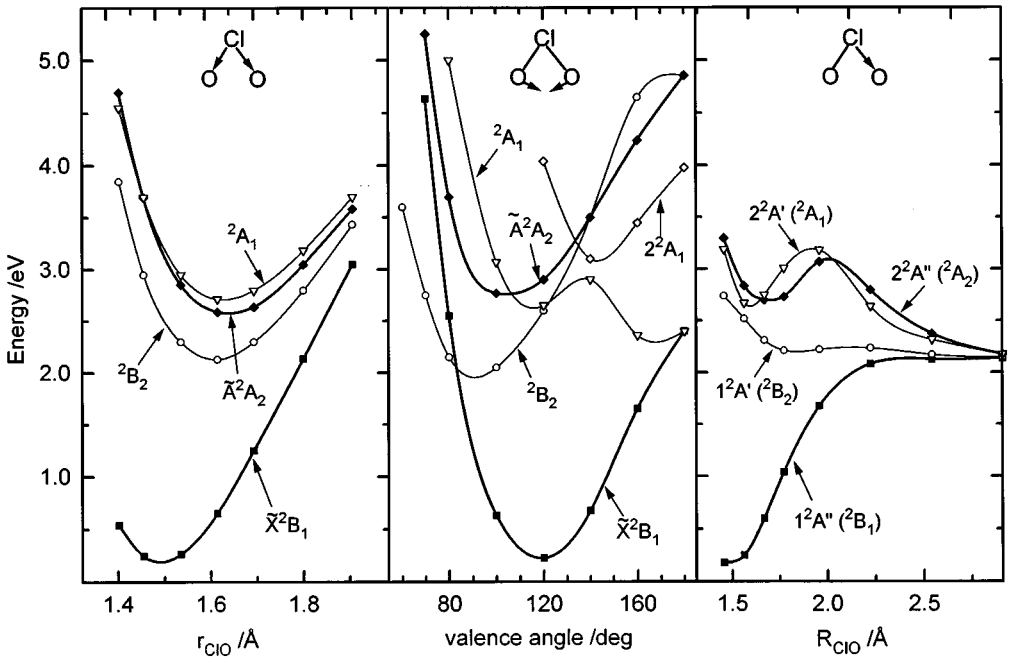

FIG. 7. Potential energy surface of several electronic states of the OClO molecule calculated by Peterson and Werner (Ref. 17). Depicted are one-dimensional cuts with respect to symmetric distortion of both Cl–O bonds (left part, valence angle fixed at 106.4°), variation of the valence angle (middle part, r_{ClO}=1.56 Å), and asymmetric bond distortion of one Cl–O bond (right part, valence angle fixed at 117.4 and r_{ClO}=1.56 Å).

Downloaded¬08¬Jan¬2002¬to¬134.169.41.178.¬Redistribution¬subject¬to¬AIP¬license¬or¬copyright,¬see¬http://ojps.aip.org/jcpo/jcpcr.jsp

increasing excitation of the ν_1 mode of the $\tilde{A}\ ^2A_2$ state [$\nu_1=6$, 7, 8 corresponds to $(\tilde{A}\ ^2A_2\nu_1,0,0)\leftarrow(\tilde{X}\ ^2B_1 0,0,0)$ excitation energies of 3.09 eV, 3.20 eV, 3.29 eV].[36] At the excitation wavelengths of our study (351 nm≡3.53 eV, 308 nm≡4.03 eV), the strongly vibrating OClO will be above the barrier and the observed ClO products could be generated via vibrational predissociation of the $\tilde{A}\ ^2A_2$ state along the ν_3 coordinate. Although the system is bound along the initially excited symmetric stretching mode ν_1, the slightest coupling between ν_1 and ν_3 is sufficient to achieve an asymmetric system and energy will be transferred into the asymmetric nuclear motion. As soon as sufficient energy is transferred into the asymmetric bond length distortion in order to overcome the barrier, the OClO molecule will decay into a vibrationally excited ClO fragment and an O atom. If the energy released in descending the exit barrier is essentially transferred into translation and rotation (but not vibration) then one would expect highly vibrating ClO products where the vibrational energy is essentially given by the energy difference between the excitation energy to reach the $\tilde{A}\ ^2A_2$ state and the total height of the barrier. Due to the angular geometry of OClO it is very likely that a simple repulsion of the O atom will essentially induce translation and rotation but only to a minor part vibration. At the photolysis wavelength of 351 nm the maximum of the ClO vibrational state distribution is found to be at $v=3$ corresponding to an energy of ~0.4 eV. This energy is the difference between the photon energy, 3.53 eV, and the total energy required to overcome the barrier, 3.1 eV. The energy barrier is supposed to be overcome the faster the higher the ν_1 mode is excited and the vibrational excitation of ClO may be attributed to the initial high vibronic excitation of the $(\tilde{A}\ ^2A_2\nu_1,0,0)$ parent molecule. As a consequence, the photodissociation of OClO at 308 nm should generate vibrationally extremely hot ClO radicals which, indeed, is observed in our experiment (Fig. 6).

A decay along ν_3 is also indicated by the observed moderate rotational excitation of the ClO radicals. The rotational state distribution of the fragments is probably initiated by the decrease of the bond angle from around 117.6° to 107° occurring in the electronic transition between $\tilde{X}\ ^2B_1$ and $\tilde{A}\ ^2A_2$ (Ref. 32) and by the repulsion on the upper potential of OClO leading to the O+ClO fragments. Vibronic coupling involving the bending mode should lead to a much higher rotational excitation of the ClO fragments than is observed in the experiment. The minimum energy of the $^2A_1$ surface with respect to the valence angle is obtained for a linear O–Cl–O. The torque which is induced on this surface by changing the valence angle from 107° (minimum on the $\tilde{A}\ ^2A_2$ surface) to 180° should result in highly rotating ClO products. According to the calculations of Peterson and Werner, the energy difference between $\tilde{A}\ ^2A_2(107°)$ and $^2A_1(180°)$ amounts to ~0.36 eV. However, the observed average ClO rotational energy is 0.08 eV (Table II).

In principle, another fundamental pathway involving coupling of the $(\tilde{A}\ ^2A_2)$ state with the $(\tilde{X}\ ^2B_1)$ ground state is possible,[27]

$$\tilde{X}\ ^2B_1(0,0,0)+h\nu\rightarrow\tilde{A}\ ^2A_2(v_1\gg 0,0,0)$$
$$\rightarrow\tilde{X}\ ^2B_1(v_1\gg 0,v_2\gg 0,v_3\gg 0)$$
$$\rightarrow \mathrm{ClO}(^2\Pi,v,J)+\mathrm{O}(^3P).$$

In this case, the intermediate is a vibrationally hot OClO molecule in the ground state. Donald and Innes[30] concluded from line width measurements that this decay channel is unlikely at low energies. However, at higher excitation energies the number of states increases considerably and the decay rate via this channel should increase.[27] A RRKM calculation of Baumert *et al.*[27] shows that the decay time decreases from 130 fs to 90 fs when the dissociation wavelength is varied from 350 nm to 310 nm.[33] This decay mechanism implies a broad energy distribution within the $\tilde{X}\ ^2B_1$ ground state and one might expect a statistical energy distribution for the ClO product. A simple prior distribution is calculated using the rigid rotator harmonic oscillator approximation (RRHO). The results (Tables I, II; 351 nm photolysis) indicate that the experimental distribution strongly deviates from this statistical distribution. The photodissociation of OClO at 308 nm leads to formation of vibrationally extremely hot ClO radicals (Fig. 6). The release of the available energy is very specific and strongly deviates from a statistical distribution. The ClO is generated essentially in very high vibrational states. The rotational excitation is rather low and comparable to that of the photolysis at 351 nm.

The formation of ClO in very high vibrational states directly explains the results of Glownia *et al.*[34] who used a femtosecond pump-and-probe experiment to observe ClO formation after OClO excitation at 308 nm. The build up time of ClO was in the order of a nanosecond. This cannot be explained by a long living intermediate but by collisional relaxation of the vibrationally excited ClO.[6]

The observed extremely high vibrational excitation of ClO at short photodissociation wavelengths may have an impact on our understanding of the atmosphere because new reaction channels are open when ClO is formed in high vibrational states. For example, the reaction of $\mathrm{ClO}+\mathrm{N_2}$ is endothermic by 8500 cm^{-1} (Ref. 35) whereas the internal energy of the ClO fragment generated in the photodissociation of OClO at 308 nm is even higher.

In summary, the photolysis at 351 nm and 308 nm excites the electronic OClO $(\tilde{A}\ ^2A_2\leftarrow\tilde{X}\ ^2B_1)$ transition with simultaneous powerful excitation of only symmetric stretching modes of the $\tilde{A}\ ^2A_2$ state. Slight disturbances provide the fast vibrational predissociation of the parent molecule on the $\tilde{A}\ ^2A_2$ $(^2A'')$ surface into the fragments, $\mathrm{ClO}(^2\Pi,v,J)+\mathrm{O}(^3P)$, of which the ClO is generated with high vibrational but only moderate rotational energy.

ACKNOWLEDGMENTS

This work was supported by the Deutsche Forschungsgemeinschaft. S. B. thanks the Konrad-Adenauer-Stiftung for fellowship support. Special thanks to T. Haas, C. Maul, and M. Roth for the recording of the very helpful REMPI/TOF spectra. We thank Professor Dr. F. J. Comes for material support and helpful discussions.

Downloaded¬08¬Jan¬2002¬to¬134.169.41.178.¬Redistribution¬subject¬to¬AIP¬license¬or¬copyright,¬see¬http://ojps.aip.org/jcpo/jcpcr.jsp

[1] S. Solomon, Nature **347**, 347 (1990).
[2] R. S. Stolarski and R. J. Cicerone, Can. J. Chem. **52**, 1582 (1974).
[3] J. G. Anderson, W. H. Brune, and M. H. Proffitt, J. Geophys. Res. **94**, 11 465 (1989).
[4] G. L. Manney, L. Froidevaux, and J. W. Waters, Nature **370**, 429 (1994).
[5] V. Vaida, S. Solomon, E. C. Richard, E. Rühl, and A. Jefferson, Nature **342**, 405 (1989).
[6] E. Rühl, A. Jefferson, and V. Vaida, J. Phys. Chem. **94**, 2990 (1990).
[7] E. Bishenden, J. Haddock, and D. J. Donaldson, J. Phys. Chem. **95**, 2113 (1991).
[8] V. Vaida, E. C. Richard, A. Jefferson, L. A. Cooper, R. Flesch, and E. Rühl, Ber. Bunsenges. Phys. Chem. **96**, 391 (1992).
[9] H. F. Davis and Y. T. Lee, J. Phys. Chem. **96**, 5681 (1992).
[10] R. Flesch, B. Wassermann, B. Rothmund, and E. Rühl, J. Phys. Chem. **98**, 6263 (1994).
[11] A. J. Colussi and S. P. Sander, Chem. Phys. Lett. **187**, 85 (1991).
[12] A. Arkell and I. Schwager, J. Am. Chem. Soc. **89**, 5999 (1967).
[13] S. Baumgärtel and K.-H. Gericke, Chem. Phys. Lett. **227**, 461 (1994).
[14] M. A. A. Clyne, I. S. McDermid, and A. H. Curran, J. Photochem. **5**, 201 (1976).
[15] Y. Matsumi, S. M. Shamsuddin, and M. Kawasaki, J. Chem. Phys. **101**, 8262 (1994).
[16] E. Bishenden and D. J. Donaldson, J. Chem. Phys. **101**, 9565 (1994).
[17] K. A. Peterson and H. J. Werner, J. Chem. Phys. **96**, 8948 (1992).
[18] R. I. Derby and W. S. Hutchinson, Inorg. Synth. **4**, 152 (1953).
[19] A. Wahner, G. S. Tyndall, and A. R. Ravishankara, J. Phys. Chem. **91**, 2734 (1987).
[20] C. Maul, M. Roth, and K.-H. Gericke (unpublished).
[21] T. Kinugawa, T. Sato, T. Arikawa, Y. Matsumi, and M. Kawasaki, J. Chem. Phys. **93**, 3289 (1990).
[22] C. Maul, T. Haas, and K.-H. Gericke, J. Chem. Phys. **192**, 3238 (1995).
[23] J. B. Nee and K. J. Hsu, J. Photochem. Photobiol. A: Chem. **55**, 269 (1991).
[24] J. A. Coxon, Can. J. Phys. **57**, 1538 (1979).
[25] K.-H. Gericke, T. Haas, M. Lock, R. Theinl, and F. J. Comes, J. Phys. Chem. **95**, 6104 (1991).
[26] S.-C. Yang and R. Bersohn, J. Chem. Phys. **61**, 460, 4400 (1974).
[27] T. Baumert, J. L. Herek, and A. H. Zewail, J. Chem. Phys. **99**, 4430 (1993).
[28] D. S. Bethune, A. J. Schell-Sorokin, J. R. Lankard, M. M. T. Loy, and P. P. Sorokin, in *Advances in Laser Spectroscopy*, edited by Garetz and Lombardi (Heyden, Philadelphia, 1983), Vol. 2, p. 1.
[29] I. P. Fischer, Trans. Faraday Soc. **63**, 684 (1967).
[30] D. A. McDonald and K. K. Innes, Chem. Phys. Lett. **59**, 562 (1987).
[31] S. Michielsen, A. J. Merer, S. A. Rice, F. A. Novak, K. A. Freed, and Y. J. Hamada, J. Chem. Phys. **74**, 3089 (1981).
[32] J. L. Gole, J. Phys. Chem. **84**, 1333 (1980).
[33] The calculated decay times just serve as an estimation of the order of magnitude.
[34] J. H. Glownia, J. Misewich, and P. P. Sorokin, in *Supercontinuum Lasers*, edited by R. R. Alfano (Springer, Berlin, 1990), p. 370.
[35] D. L. Baulch, R. A. Cox, R. F. Hampson, Jr., J. A. Kerr, J. Troe, and R. T. Watson, J. Phys. Chem. Ref. Data **13**, 1259 (1984).
[36] E. C. Richard and V. Vaida, J. Chem. Phys. **94**, 163 (1990).

Downloaded¬08¬Jan¬2002¬to¬134.169.41.178.¬Redistribution¬subject¬to¬AIP¬license¬or¬copyright,¬see¬http://ojps.aip.org/jcpo/jcpcr.jsp